DOI 10.5012/bkcs.2009.30.12.3039

Electric Field Dependence Experiments and ab Initio Calculations of Three Cytosine Tautomers in Superfluid Helium Nanodroplets

Ahreum Min, Seung Jun Lee, Myong Yong Choi,* and Roger E. Miller†‡

Department of Chemistry and Research Institute of Natural Science, Gyeongsang National University, Jinju 660-701, Korea
**E-mail: mychoi@gnu.ac.kr*
†Department of Chemistry, The University of North Carolina at Chapel Hill, Chapel Hill, North Carolina 27599, U. S. A.
‡Deceased. November 6, 2005
Received September 25, 2009, Accepted October 26, 2009

We report the first electric field dependence IR spectra of three cytosine tautomers solvated in helium nanodroplets. By using an electric field dependence on the three lowest energy tautomers of cytosine and ab initio calculations, we are able to measure the vibrational transition moment angles (VTMAs), specifically for the NH_2 symmetric stretch (SS) mode in this study, with more precision; thus we have reassigned the previous NH_2 (SS) VTMA of 74° for the C1 tautomer to 85°, which the latter is in excellent agreement with the ab initio value. Nonplanarity of the three lowest energy tautomers of cytosine has been investigated by measuring the VTMA of each vibrational mode for the tautomers.

Key Words: Superfluid helium droplets, Cytosine tautomers, Vibrational transition moment angle (VTMA), Pendular spectroscopy, ab Initio and DFT calculations

Introduction

Usually the structural information of isolated molecules is obtained from the rotational constants by rotational spectroscopy; however, for nucleic acid bases (NABs), their structural information is obscured with difficulty of obtaining the rotational constants due to the high melting point and thermal instability of NABs. Recently, therefore, there have been enormously large efforts on investigating the structures of biologically important molecules *via* vibrational spectroscopy with an aid of quantum mechanical calculations.[1-6] Among them, the application of pendular spectroscopy has been one of the important techniques, which orients molecules in the laboratory frame for photodissociation,[7,8] cross molecular beam[9-12] and helium nanodroplet experiments.[13-16] In the latter, using low temperature (0.4 K) characteristic of helium nanodroplets and the pendular spectroscopy, polar molecules in a high DC electric field become oriented in the laboratory frame, such that the angle between the permanent dipole and transition dipole moments, called vibrational transition moment angle (VTMA), is experimentally obtained.[1,17-25]

In the previous reports on the VTMA measurements of cytosine,[18] we employed vibrational spectroscopy of cytosine solvated in helium nanodroplets to identify the three lowest energy tautomers, namely C1, C31 and C32, with an assist of measuring the vibrational transition moment angles (VTMAs) of high frequency O-H, N-H and NH_2 stretches of each tautomer as well as the ab initio frequency calculations. Along with the VTMA study of adenine, we further investigated the nonplanarity of adenine by comparing the VTMAs of experimental and calculated values which the latter were obtained by varying the dihedral angles associated with the NH_2 groups. In the study of adenine, we have confirmed that the VTMAs are very sensitive to the structure of molecules.[23]

In the present experiment, in addition to the same techniques mentioned above, we apply a recently developed method[23] for a polar molecule's orientation in the high electric field to the cytosine tautomer system. The excitation efficiency of cytosine tautomers is dependent upon the several different parameters, such as permanent and transition dipole moments, DC electric field and VTMA. By using this method, we have reanalyzed the NH_2 symmetry stretch (SS) band of cytosine tautomers. Furthermore, we discuss the nonplanarity of each cytosine tautomer by freezing the dihedral angle of the NH_2 group with respect to the VTMA changes of the N(O)-H, NH_2 asymmetric and symmetric modes.

Experimental Section

The experimental apparatus has been described elsewhere in detail,[26,27] thus only a brief explanation is provided in this paper. Nanodroplets with a mean size of 3,000 helium atoms were formed by expanding ultrahigh purity helium (99.9999%) from a 5 μm diameter orifice, operated at 50 atm pressure and a temperature of 20.5 K. Cytosine was doped to the droplets by pick-up[28] in a scattering-box oven, the temperature of which was optimized for the capture of a single molecule (~ 210 °C). Upon being captured by the droplets, cytosine is quickly cooled to the 0.37 K temperature of the droplets at typical rates of 10^{10} K/s.[29]

In this work, using a periodically poled lithium niobate optical parametric oscillator (cw-PPLN-OPO) from Linos Photonics, the IR laser beam is directed into a multipass cell,[26] used to improve the excitation efficiency by having multiple crossings between the laser and droplet beams. Vibrational excitation of the solvated molecules results in the evaporation of several hundred helium atoms. The resulting laser induced decrease in the kinetic energy of the droplet beam is detected by a bolometer, which is positioned downstream of the laser interaction region. The laser beam is amplitude modulated and a phase sensitive

detection of the bolometer signal is used to improve the signal-to-noise ratio. A series of external etalons and a wavemeter were used to calibrate the resulting infrared spectra.

For orienting a solvated polar molecule, two stark electrodes are positioned on either side of the laser interaction region. The laser electric field direction is then aligned either parallel or perpendicular to the DC electric field, which we have applied up to about 80 kV/cm in this study.

VTMAs and ab Initio Calculations

The orientation of polar molecules in the laboratory fixed frame has several important advantages,[13-16,30] in which we have used this as a structural tool for biologically important molecules and further for their water complexes.[1,18-25] In this study, at the low temperature (0.37 K),[29] associated with helium nanodroplets, and large electric field (65 kV/cm), strong orientation of the molecules was achieved since the interaction between the dipole moment and the DC electric field is much larger than the rotational energy. The experimental measurement of the ratio of the integrated areas, namely the polarization ratio as a function of α, for a given vibrational mode with the laser polarization aligned parallel and perpendicular to the applied electric field is shown below.

$$\rho(\alpha) = \frac{A_{\parallel}(\alpha)}{A_{\perp}(\alpha)} \quad (1)$$

$$= \frac{2\int_0^{\pi} P(\cos\theta)[2\cos^2\theta + \sin^2\alpha - 3\cos^2\theta\sin^2\alpha]\sin\theta d\theta}{\int_0^{\pi} P(\cos\theta)[2 - \sin^2\alpha - 2\cos^2\theta + 3\cos^2\theta\sin^2\alpha]\sin\theta d\theta}$$

where, θ is the angle between the permanent dipole moment direction and the Z-axis, defined as the direction of the applied field. The normalized orientation distribution is then given by $P(\cos\theta)$, namely:

$$P(\cos\theta) = \int_0^{2\pi} P(\cos(\theta,\varphi))d\varphi = \tfrac{1}{2}(1 + \sum_{n=1}^{\infty} a_n P_n(\cos\theta)) \quad (2)$$

This distribution depends upon the magnitude of the dipole moment, the applied electric field, the rotational constants, and temperature of the molecule in question. The methods for calculating this distribution have been discussed by Kong's group in detail previously.[31-33]

The experimental VTMAs (α) are determined from Equation (1) by measuring the ratio of the integrated band intensities for parallel and perpendicular polarization, normalized using the corresponding field free spectra. These angles can also be extracted from ab initio calculations for direct comparison with the experimental values.[1] The calculated VTMAs were obtained by using the Moller-Plesset perturbation theory at the 2nd order (MP2) level and density functional theory (DFT) calculations at a Becke's three parameters hybrid functional method (B3LYP) with a 6-311++G(d,p) basis set using Gaussian 03.[34] Figure 1 shows the structure of cytosine tautomers, C31, C32 and C1, with the ab initio transition moment vectors (empty

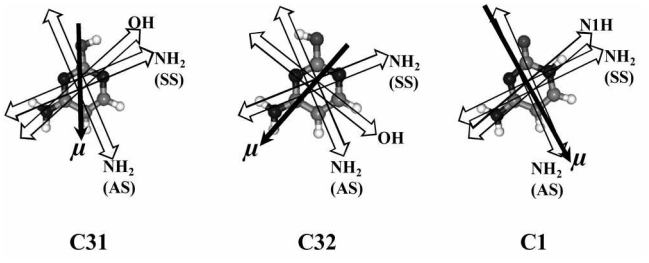

Figure 1. The three lowest energy tautomers of cytosine, showing the corresponding directions of the permanent electric dipole moments (the length of the solid arrow is proportional to the dipole magnitudes) and the vibrational transition moments (empty double ended arrows) for the various vibrational modes. The magnitudes of these moments are given in Table 1.

Table 1. Experimental and calculated data for the VTMA analysis of the various cytosine tautomers

				MP2[a]				DFT[b]			
tauto-meter	assign-ment	exp. freq. (cm^{-1})	exp. VTMA(°)	ab initio VTMA(°)	rotational constant (cm^{-1})	μ_p (debye)	relative[c] energy (kJ/mol)	DFT VTMA(°)	rotational constant (cm^{-1})	μ_p (debye)	relative[c] energy (kJ/mol)
C31						3.39	0.0			3.46	4.9
	OH	3609.7	43	47	A = 0.1312	x = -2.80		41	A = 0.1320	x = 3.10	
	NH_2(AS)	3572.3	22	26	B = 0.0667	y = 1.71		27	B = 0.0669	y = 1.46	
	NH_2(SS)	3455.9	66	70	C = 0.0443	z = 0.87		66	C = 0.0444	z = 0.50	
C32						4.56	3.0			4.81	8.1
	OH	3617.9	81	88	A = 0.1293	x = 4.41		89	A = 0.1297	x = 4.67	
	NH_2(AS)	3570.9	61	64	B = 0.0672	y = -0.79		63	B = 0.0675	y = -1.07	
	NH_2(SS)	3457.2	29	29	C = 0.0443	z = 0.88		27	C = 0.0444	z = 0.54	
C1						6.38	7.8			6.75	0.0
	NH_2(AS)	3572.7	12	6	A = 0.1286	x = 3.80		7	A = 0.1289	x = 4.41	
	H1H	3471.7	71	78	B = 0.0671	y = 5.06		72	B = 0.0674	y = 5.10	
	NH_2(SS)	3451.7	85(74)[d]	88	C = 0.0441	z = 0.78		84	C = 0.0443	z = 0.36	

[a]The ab initio calculations were performed at the MP2/6-311--G(d,p) level. [b]The DFT calculations were performed at the B3LYP/6-311++G(d,p) level. [c]The energy was obtained with zero point energy corrections. [d]The value in the parentheses is from the previous work.[18]

double ended arrows) and permanent electric dipole moments (solid arrows) superimposed on the molecules. Detailed information about the ab initio VTMAs and relative equilibrium energies of the tautomers in Figure 1 is listed in Table 1.

Results and Discussion

In the previous study of cytosine,[18] we showed a survey scan of 3325 - 3700 cm^{-1} region and assigned all major bands to the NH_2 asymmetric stretching (AS), N-H and NH_2 symmetric stretching (SS) modes of the C31, C32 and C1 tautomers. The assignment was achieved with a comparison between the measurement of VTMAs and the ab initio VTMA calculations. Even though the assignment was conclusive with the analysis of VTMAs and ab initio calculations, there was a mismatch in the VTMA of NH_2 (SS) band of C1 between the experimental and ab initio value. Therefore, we further investigated the experimental and theoretical VTMA analysis of major three cytosine tautomers.

As described above, we calculated the rotational constants, A, B and C, for the each cytosine tautomer since the obtained band spectrum was not rotationally resolved. The resulting rotational constants and the permanent dipole moment, μ_p, for the isolated molecules are listed in Table 1. The ab initio and DFT rotational constants were modified to account for the effect of the helium solvent in the VTMA analysis.[35] Therefore, the rotational constants were decreased by a factor of three upon solvation in helium.[35] Here we have to mention that the orientation distributions are very weakly dependent on the values of the rotational constants at the fields used in this experiment. As a result, we conducted the VTMA analysis by assuming that the rotational constants are the ab initio values divided by a factor of three.

The experimental VTMAs of C31, C32 and C1 can be obtained from the curves in Figure 2, which shows the polarization ratios, $\rho(\alpha)$, obtained from equation (1). For the case of C31, shown in Figure 2 (a), the ab initio constants μ_p = 3.39 debye, A = 0.1312, B = 0.0667, C = 0.0443 cm^{-1} were used to determine the dipole distribution function, $P(\cos\theta)$, equation (2), resulting in the dashed curve for $\rho(\alpha)$. The dashed and solid curves were calculated using the ab initio rotational constants without and with reducing the rotational constants by a factor of three, respectively, as mentioned above. Even if the rotational constant correction factor is changed by a factor of three, only a small change in the polarization ratio is observed with more change for more parallel bands. Very similarly, the VTMAs of C32 (b) and C1 (c) were also determined in Figure 2.

The results of this analysis are summarized in Table 1. It is worth mentioning that the experimental VTMA of NH_2 (SS) for C1 was previously 74°,[18] however, it turned out to be 85° ± 5° after reanalysis of the band, much close to the ab initio value of 88°, which will be discussed later. Overall, the experimental and calculated VTMAs, including DFT calculations, are in excellent agreement for the cytosine tautomers.

Figure 3 (a) shows the expanded region of the NH_2 (SS) modes of the cytosine tautomers, recorded as a function of the sample oven temperatures. The normalized integrated band intensities of each band are plotted in Figure 3 (b), in which the bands marked with "*" and "#" tend to disappear at lower

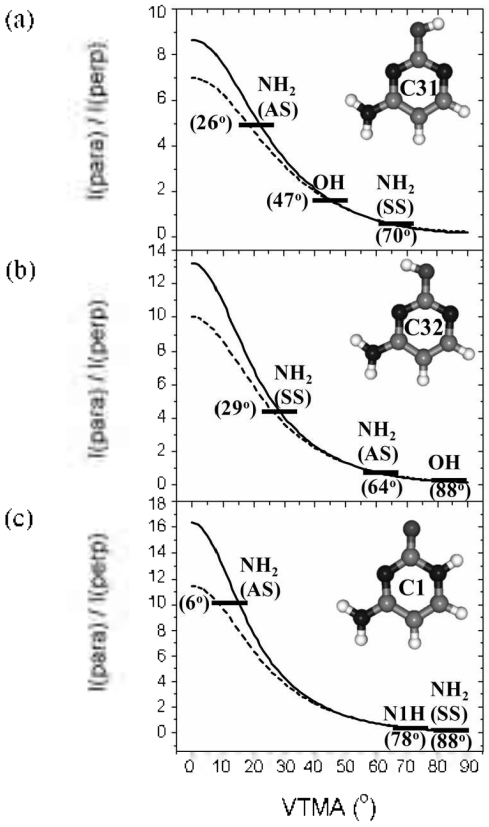

Figure 2. The integrated intensity ratio, $\rho(\alpha)$, calculated from equation (1) in the text for C31 (a), C32 (b) and C1 (c). The solid and dashed curve was generated using the ab initio rotational constants (see Table 1) with and without reducing the rotational constants by a factor of three, respectively. The predicted VTMAs obtained at the MP2/6-311++G(d,p) level of theory are included in parentheses. The horizontal lines are the measured intensity ratios for the corresponding vibrational modes.

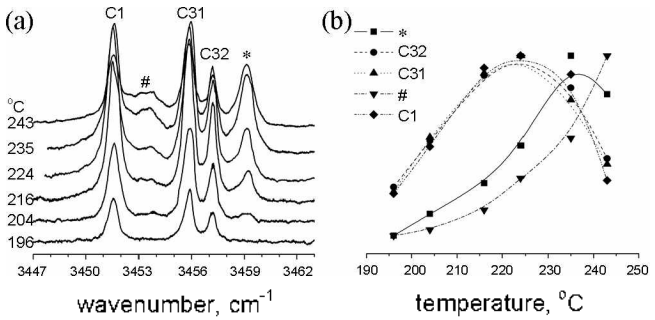

Figure 3. An oven temperature dependence of NH_2 (SS) mode region (a) and the normalized intensity plots for the corresponding bands (b). The three major cytosine tautomers clearly optimizes at lower temperatures, consistent with the fact that lower vapor pressures are required for the pick-up of a single molecule. The other bands marked with "*" and "#" are tentatively assigned to the dimers and trimers due to the fact that they require higher vapor pressures for optimum signals.

oven temperatures, while the other three bands show almost similar band intensities as a function of oven temperatures. Indeed, we assign the bands marked with "*" and "#" are attributed to the cytosine complexes, such as dimers and trimers, respectively.

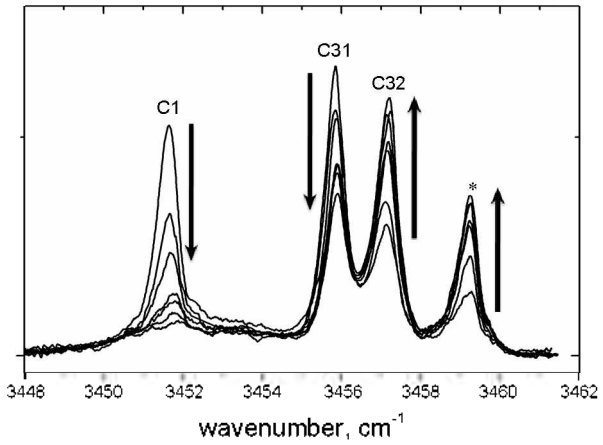

Figure 4. Electric field dependence spectra of the NH_2 (SS) band region of the C31, C32 and C1 tautomer at parallel polarization. As the field increases, the parallel and perpendicular band intensity increases and decreases, respectively. The magnitude of intensity change is dependent upon the several parameters, mentioned in the text. The band mark with "*" is due to the cytosine dimer.

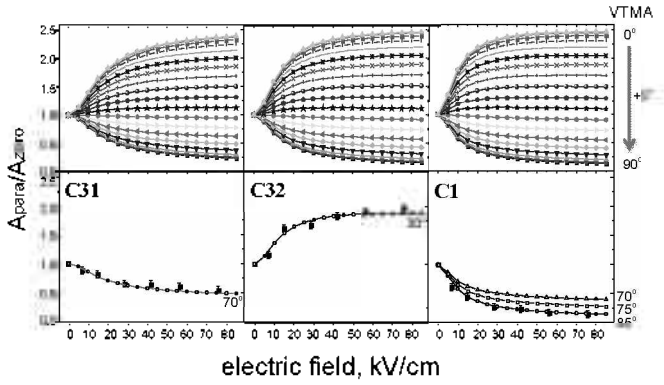

Figure 5. Calculated polarization ratios, $A_{(para)}/A_{(zero)}$, in upper panels, of the NH_2 (SS) modes for the C31, C32 and C1 tautomers with increasing the electric field, from 0° to 90° with a 5° gap, between the two Stark electrodes. The ab initio constants for each tautomer, dipole moments and rotational constants, listed in Table 1, were used in the calculations. The graphs clearly show that the curvature of the polarization ratio with different dipole moments at especially low electric fields is very distinctive. The down panels show comparisons between the ab initio polarization ratio curve (open shapes with a line) and experimental polarization ratio (filled squares with error bars) of C31, C32 and C1. The numbers in the down panels represent the ab initio polarization curves for the corresponding VTMA values.

Compared to the other two vibrational modes, NH_2 (AS) and N-H, of the cytosine tautomers, the NH_2 (SS) mode of the C31 and C32 and C1 tautomer is well separated as shown in Figure 3 and listed in Table 1. For the case of NH_2 (AS) mode, the frequencies of C31 and C32 tautomers lie almost within one wavenumber, (see Table 1) making rather difficult to analyze the electric field dependence polarization ratio curves. Therefore, we focused on the electric field and laser polarization direction dependence of the NH_2 (SS) bands for the cytosine monomers, C31, C32 and C1. Figure 4 shows the electric field dependence of the NH_2 (SS) vibrational bands with 0, 7.1, 14.8, 28.5, 41.9, 56.3, 75.8 kV/cm at parallel polarization field. The perpendicular band, 88 and 70°, of C1 and C31 decreases as the electric field increases while the parallel band, 29°, of C32 increases. Here it is interesting to note that the trend of increasing and decreasing band intensity is quite different from each other, for example, the decrease of C1 is more rapid than that of C31, which is due to the larger values of VTMA and dipole moment of C1 than those of C31. This was well discussed in the recent study of guanine tautomers.[21] Further investigation of this matter is discussed below.

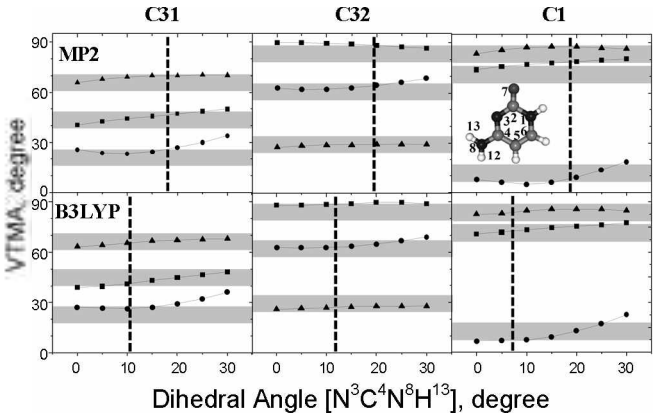

Figure 6. The evolution of VTMAs of C31, C32, and C1 as a function of the dihedral angle, $N^3C^4N^8H^{13}$, from 0 to 30°, using a 6-311++G(d,p) basis set with an MP2 (upper panels) and B3LYP (down panels) level of theory. The vertical lines in upper panels show that the dihedral angle, $N^3C^4N^8H^{13}$, of the optimized structure of C31, C32 and C1 is 18°, 19° and 18°, respectively, with an MP2 level of theory, while that with a B3LYP (down panels) is 10°, 12° and 7°, respectively. The horizontal thick lines indicate the experimental VTMAs of the corresponding vibrational bands of C31, C32 and C1. The thickness of the line shows the experimental error limit (± 5°). The circles, triangles and squares indicate the calculated VTMAs of the vibrational bands, NH_2 (AS), NH_2 (SS) and N(O)H, respectively.

The upper panels of Figure 5 show the plots of calculated polarization ratio, $A_{parallel}/A_{zero}$, for the NH_2 (SS) bands of the three tautomers with increasing the electric field between the two stark electrodes for 19 different (0 - 90° with a 5° gap) ratios. A molecule with a larger dipole moment requires a smaller electric field for complete orientation, while much larger fields are needed to reach this saturation condition if the dipole moment is smaller. This is well illustrated in Figure 5, for example, for the case of C31 (3.4 debye) and C1 (6.4 debye), of which the later showed a steeper slope at the VTMAs of 0 and 90°. The down panels show the comparisons between experimental (filled squares with error bars) and calculated (open shapes with a line) values of the polarization ratio for the NH_2 (SS) bands of C31, C32 and C1 as a function of electric field strength. The ab initio polarization ratio curves of 70° (C31) and 30° (C32) are in excellent agreement with the experimental ratio of integrated areas, $A_{parallel}/A_{zero}$. The experimental VTMAs of 66 and 29° for the C31 and C32 tautomers, respectively, further support the agreement. However, the previous experimental VTMA assignment of C1, 74°, was deviated from the ab initio polarization ratio curves of 70 and 75°. It is rather very close to the ab initio curve of 85° and the ab initio VTMA value of 88° as well. This discrepancy between the values from the same group

might be due to increased errors in the integration of the band intensities subject to the experimental polarization ratio (A_{para}/A_{perp}) contributed from the background on the high frequency shoulder of the band, as shown in Figure 3(a). There may be some perpendicular band contributions from high order clusters in the VTMA, however, in the present electric field dependence experiment; we have used the integrated intensity ratio of parallel over zero field, instead of perpendicular field. Very similar case was also reported in the previous VTMA study of thymine and uracil in helium nanodroplets.[22]

Up to now, we have focused on the polarization dependence of NH_2 (SS) bands of three lowest energy tautomers, presenting a quite good agreement between theory and experiment. Now we begin to discuss the VTMA change with respect to tilting a dihedral angle of NH_2 group. We calculated the VTMAs of three vibrational modes of C31, C32 and C1 by freezing the dihedral angle of $N^3C^4N^8H^{13}$ while the other atoms are fully relaxed, shown in Figure 6. The calculations were done at the DFT and MP2 level of theory with a 6-311++G(d,p) basis set. It is well known that the VTMAs of vibrational modes are very stable compared to the stability of ab initio frequencies of each vibrational bands upon different basis sets, suggesting that quantitative comparisons can be made with experiment even using very modest ab initio calculations.[23,25] This is important when applying these techniques to much larger systems, where large basis sets may be prohibitively expensive. The reason for the insensitivity of the VTMAs to basis set size can be appreciated by noting that, for the localized vibrations considered here, the transition dipole moment directions are primarily determined by bond directionality.[1] Therefore, as long as the calculated structure is good, the directions of the permanent and transition moments will be rather well determined.

The upper and lower panels in Figure 6 show that the VTMAs of each vibrational mode vary as a function of the dihedral angle, $N^3C^4N^8H^{13}$, at the MP2 and B3LYP calculations, respectively. The horizontal thick lines are the experimental VTMAs of each vibrational mode with an error, ± 5°. Unfortunately, not likely to the study of adenine,[23,25] where the VTMAs vary significantly with the dihedral angle, they are vey muted (within the error limit) with the angles for the case of cytosine. Therefore, the detailed structural information about the nonplanarity of cytosine cannot be obtained in this study. It is, however, interesting to note that nonplanarity of cytosine tautomers was not dependent upon the level of theory used in this study, both predicting a nonplanar structure, supported by the vertical dotted lines, the angles obtained from full geometry optimizations. Nonetheless, the structures of adenine showed a strong dependence on the type of theory, MP2 and B3LYP, which predicted a nonplanar and planar structure, respectively.[23,25] It still, however, shows that more nonplanar structures of cytosine tautomers are predicted from the MP2 than from DFT calculations, similar to the nonplanarity study of adenine.

Summary

In this study we have presented the first electric field dependence of IR spectra of cytosine isolated in superfluid helium nanodroplets. By varying a DC electric field to the polar molecules, the different permanent dipole moments of system induced different orientation behavior with respect to the polarization and electric field intensity. Using the recently developed technique by this group and more precise measurement of the band ratio, we have reanalyzed the measurement of VTMA for the NH_2 (SS) mode of C1. 85° ± 5° rather than 74° ± 5°, previously measured in this group. The new value is in excellent agreement with the ab initio value, 88°. Other bands are in good agreement between experiments, both the VTMA and dipole moment curve measurement, and theory.

We have attempted to characterize the nonplanarity of cytosine monomers with an aid of the experimental VTMAs of each vibrational band as in the case of adenine. Contrast to the nonplanarity study of adenine, the experimental VTMA change as a function of the dihedral angle, $N^3C^4N^8H^{13}$, were almost within the experimental error limits. Therefore, it was not able to conduct the experimental evaluation for the nonplanarity of cytosine in this study. However, a detailed VTMA study of the cytosine tautomers using both DFT and MP2 level of theory revealed that they have a nonplanar structure with full geometry optimizations, of which the geometry of adenine from DFT calculations was planar in the previous study. Based on this, it will be interesting to compare the nonplanarity of purines and pyrimidines in future studies.

Acknowledgments. This work is supported by the Korea Research Foundation Grant funded by the Korean Government (KRF-2008-313-C00396), in which main calculations were performed by using the supercomputing resource of the Korea Institute of Science and Technology Information (KISTI) and the Korean Science and Engineering Foundation (KOSEF) grant funded by the Korea government (MEST) (No. R01-2008-000-20002-0(2008)).

References

1. Dong, F.; Miller, R. E. *Science* **2002**, *298*, 1227.
2. Callahan, M. P.; Crews, B.; Abo-Riziq, A.; Grace, L.; de Vries, M. S.; Gengeliczki, Z.; Holmes, T. M.; Hill, G. A. *Phys. Chem. Chem. Phys.* **2007**, *9*, 4587.
3. Mons, M.; Piuzzi, F.; Dimicoli, I.; Gorb, L.; Leszczynski, J. *J. Phys. Chem. A* **2006**, *110*, 10921.
4. Dian, B. C.; Longarte, A.; Zwier, T. S. *Science* **2002**, *296*, 2369.
5. Bakker, J. M.; Compagnon, I.; Meijer, G.; von Helden, G.; Kabelac, M.; Hobza, P.; de Vries, M. S. *Phys. Chem. Chem. Phys.* **2004**, *6*, 2810.
6. Kim, H. M.; Han, K. Y.; Park, J.; Kim, S. K.; Kim, Z. H. *J. Chem. Phys.* **2008**, *128*, 184313/1.
7. Miller, R. E. *J. Phys. Chem.* **1986**, *90*, 3301.
8. Nahler, N. H.; Reinhard, B.; Udo, B.; Zsolt, B.; Gerber, R. B.; Bretislav, F. *J. Chem. Phys.* **2003**, *119*, 224.
9. Beuhler, R. J.; Bernstein, R. B.; Kramer, K. H. *J. Am. Chem. Soc.* **1966**, *88:22*, 5331.
10. Brooks, P. R. *Science* **1976**, *193*, 11.
11. Parker, D. H.; Jalink, H.; Stolte, S. *J. Phys. Chem.* **1987**, *91*, 5427.
12. Oudejans, L.; Miller, R. E. *J. Chem. Phys.* **2000**, *113*, 971.
13. Nauta, K.; Miller, R. E. *Phys. Rev. Lett.* **1999**, *82*, 4480.
14. Moore, D. T.; Oudejans, L.; Miller, R. E. *J. Chem. Phys.* **1999**, *110*, 197.
15. Nauta, K.; Miller, R. E. *Science* **1999**, *283*, 1895.
16. Nauta, K.; Moore, D. T.; Stiles, P. L.; Miller, R. E. *Science* **2001**, *292*, 481.
17. Douberly, G. E.; Miller, R. E. *J. Phys. Chem. B* **2003**, *107*, 4500.

18. Choi, M. Y.; Dong, F.; Miller, R. E. *Phil. Trans. R. Soc. A* **2005**, *363*, 393.
19. Choi, M. Y.; Miller, R. E. *Phys. Chem. Chem. Phys.* **2005**, *7*, 3565.
20. Choi, M. Y.; Miller, R. E. *J. Phys. Chem. A* **2006**, *110*, 9344.
21. Choi, M. Y.; Miller, R. E. *J. Am. Chem. Soc.* **2006**, *128*, 7320.
22. Choi, M. Y.; Miller, R. E. *J. Phys. Chem. A* **2007**, *111*, 2475.
23. Choi, M. Y.; Dong, F.; Han, S. W.; Miller, R. E. *J. Phys. Chem. A* **2008**, *112*, 7185.
24. Choi, M. Y.; Miller, R. E. *Chem. Phys. Lett.* **2009**, *477*, 276.
25. Lee, S. J.; Choi, M. Y.; Miller, R. E. *Chem. Phys. Lett.* **2009**, *475*, 24.
26. Nauta, K.; Miller, R. E. *J. Chem. Phys.* **1999**, *111*, 3426.
27. Choi, M. Y.; Douberly, G. E.; Falconer, T. M.; Lewis, W. K.; Lindsay, C. M.; Merritt, J. M.; Stiles, P. L.; Miller, R. E. *Int. Rev. Phys. Chem.* **2006**, *25*, 15.
28. Gough, T. E.; Mengel, M.; Rowntree, P. A.; Scoles, G. *J. Chem. Phys.* **1985**, *83*, 4958.
29. Hartmann, M.; Miller, R. E.; Toennies, J. P.; Vilesov, A. *Phys. Rev. Lett.* **1995**, *75*, 1566.
30. Block, P. A.; Bohac, E. J.; Miller, R. E. *Phys. Rev. Lett.* **1992**, *68*, 1303.
31. Franks, K. J.; Li, H. Z.; Kong, W. *J. Chem. Phys.* **1999**, *110*, 11779.
32. Castle, K. J.; Abbott, J.; Peng, X.; Kong, W. *J. Chem. Phys.* **2000**, *113*, 1415.
33. Kong, W.; Bulthuis, J. *J. Phys. Chem. A* **2000**, *104*, 1055.
34. Frisch, M. J.; Trucks, G. W.; Schlegel, H. B.; Scuseria, G. E.; Robb, M. A.; Cheeseman, J. R.; Montgomery, J. J. A.; Vreven, T.; Kudin, K. N.; Burant, J. C.; Millam, J. M.; Iyengar, S. S.; Tomasi, J.; Barone, V.; Mennucci, B.; Cossi, M.; Scalmani, G.; Rega, N.; Petersson, G. A.; Nakatsuji, H.; Hada, M.; Ehara, M.; Toyota, K.; Fukuda, R.; Hasegawa, J.; Ishida, M.; Nakajima, T.; Honda, Y.; Kitao, O.; Nakai, H.; Klene, M.; Li, X.; Knox, J. E.; Hratchian, H. P.; Cross, J. B.; Adamo, C.; Jaramillo, J.; Gomperts, R.; Stratmann, R. E.; Yazyev, O.; Austin, A. J.; Cammi, R.; Pomelli, C.; Ochterski, J. W.; Ayala, P. Y.; Morokuma, K.; Voth, G. A.; Salvador, P.; Dannenberg, J. J.; Zakrzewski, V. G.; Dapprich, S.; Daniels, A. D.; Strain, M. C.; Farkas, O.; Malick, D. K.; Rabuck, A. D.; Raghavachari, K.; Foresman, J. B.; Ortiz, J. V.; Cui, Q.; Baboul, A. G.; Clifford, S.; Cioslowski, J.; Stefanov, B. B.; Liu, G.; Liashenko, A.; Piskorz, P.; Komaromi, I.; Martin, R. L.; Fox, D. J.; Keith, T.; Al-Laham, M. A.; Peng, C. Y.; Nanayakkara, A.; Challacombe, M.; Gill, P. M. W.; Johnson, B.; Chen, W.; Wong, M. W.; Gonzalez, C.; Pople, J. A. Revision C.02 ed.; Gaussian, Inc.; Wallingford CT, 2004.
35. Callegari, C.; Lehmann, K. K.; Schmied, R.; Scoles, G. *J. Chem. Phys.* **2001**, *115*, 10090.